



BIOLOGICAL
CRYSTALLOGRAPHY

Volume 70 (2014)

Supporting information for article:

Structural and functional insights of an archaeal L-asparaginase obtained through linker-less assembly of constituent domains

Rachana Tomar, Pankaj Sharma, Ankit Srivastava, Saurabh Bansal, Ashish and Bishwajit Kundu

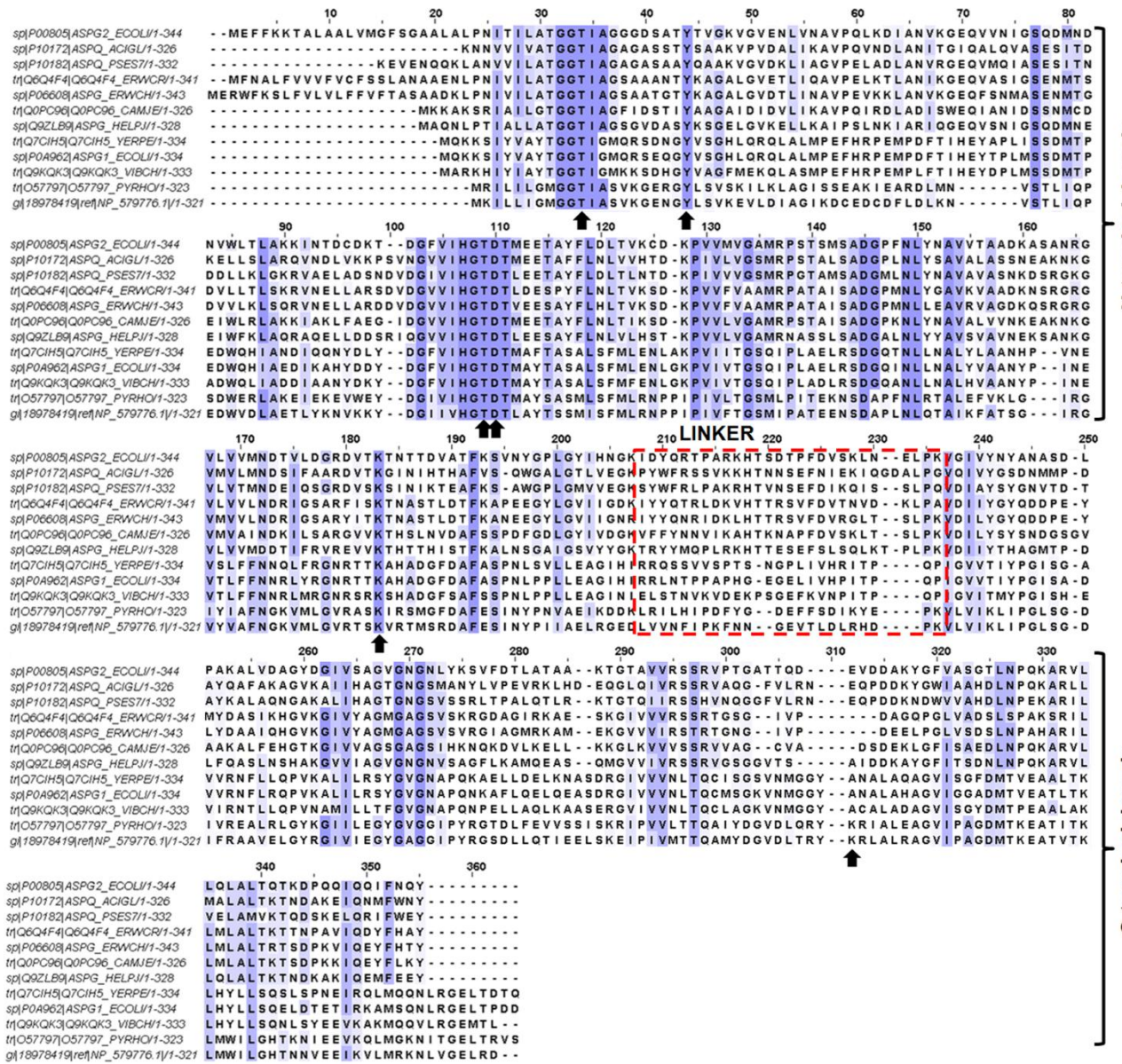


Figure S1 Sequence alignment of bacterial and archeal L-asparaginases. The alignments were produced using ClustalW2 (Thompson et al., 1994). The numbering corresponds to EcAII sequence (P0085). Identical amino acid residues are shown in blue color. The completely conserved residues are shown in dark blue. The active-site residues are marked with black arrows. The domains are marked with black brackets and the linker region is shown in dashed box (red). This figure was drawn using Jalview 2 (Waterhouse et al., 2009). The representative abbreviations are: AcA-*A. glutaminasificans* (P10172), PsA-*Pseudomonas sp.* (P10182), EcrA-*E. carotovora* (Q6Q4F4), ErAII- *E. chrysanthemi* (P06608), CjA-*C. jejuni* (Q0PC96), HpA-*H. pylori* (Q9ZLB9), EcAII-*E. coli* (P0085), PfA-*P. furiosus* (NP_579776.1), PhA-*P. horikoshii* (O57797), YpA-*Y. pestis*(Q7CIH5), EcAI-*E. coli* (P0A962), VcA-*V. cholerae* (Q9KQK3).

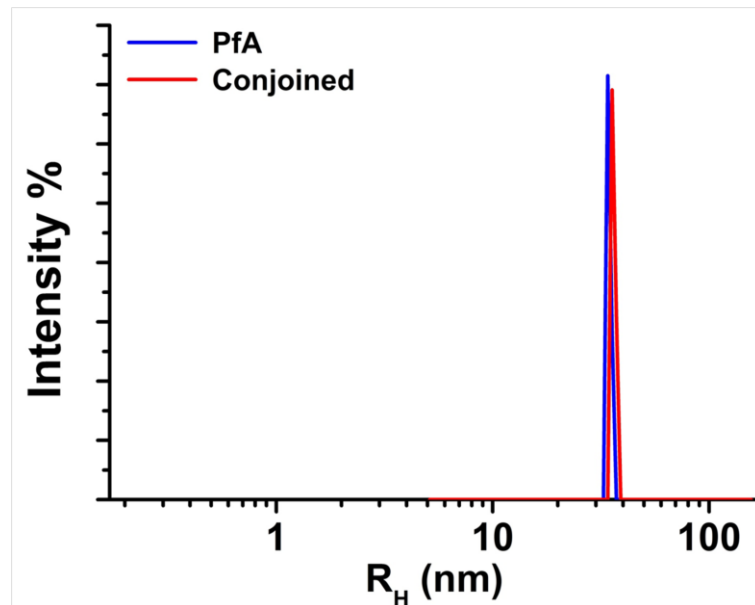


Figure S2 Dynamic light scattering profiles showing significant similarity in hydrodynamic volume of the WT and conjoined PfA.

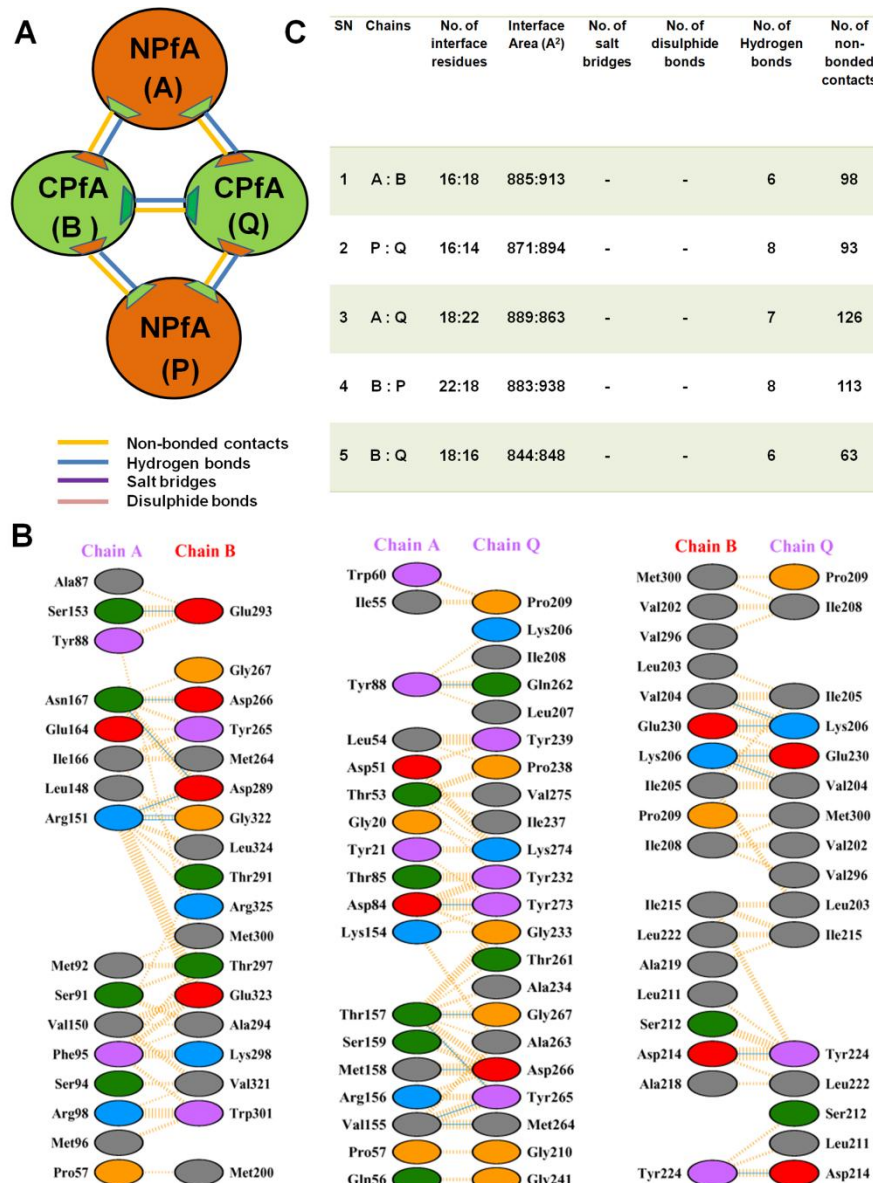


Figure S3 Interaction analysis at domain interface in conjoined PfA. **(A)** Schematic diagram showing interactions (colour coded) at domain interface among different chains. **(B)** Residues involved in interfacial interactions, Positively charged (Blue), Negative charged (Red), Neutral (Green), Aliphatic (Grey), Aromatic (Purple), Pro and Gly (Dark yellow) and Cysteine (light yellow). **(C)** Parameters calculated for interfacial interactions are given in the table.

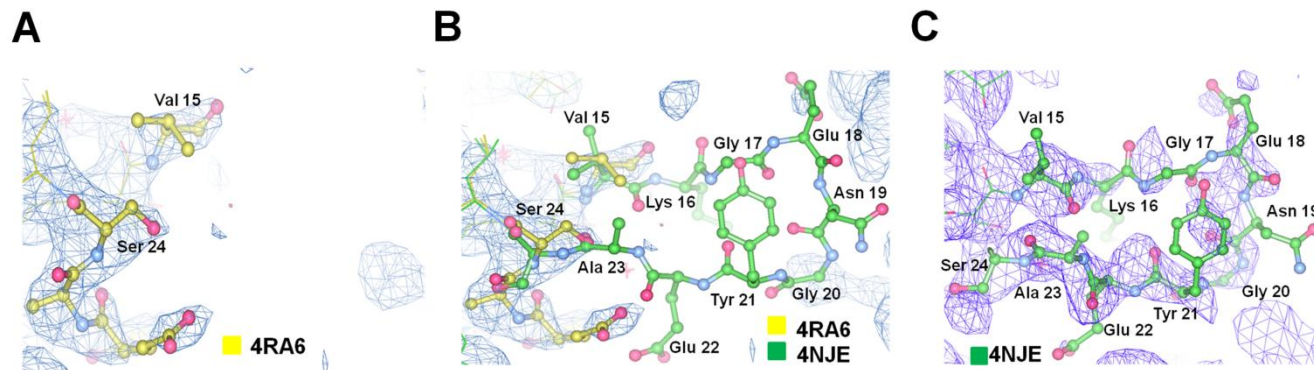


Figure S4 Flexibility of active site loop as shown by electron density 2Fo-Fc maps at above 1σ level. **(A)** Absence of electron density (mesh) in the loop region of L-asparaginase structure where substrate is not bound to the enzyme (PDB id: 4RA6). **(B)** Active site loop of substrate-bound L-asparaginase (PDB id: 4NJE) structure superimposed on substrate-free (PDB id: 4RA6) structure. **(C)** Presence of electron density at the active site loop as it gains rigidity on binding of substrate at the active site L-Asparaginase (PDB id: 4NJE).

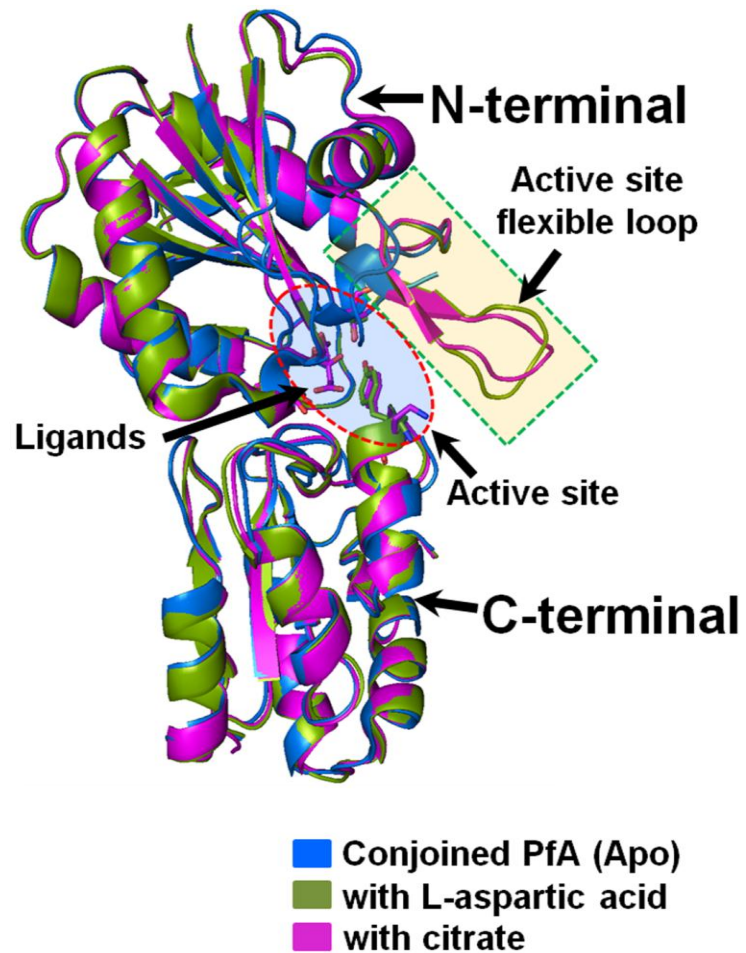


Figure S5 Ribbon diagram showing superimposed structures of conjoined PfA without ligand (Blue) (PDB id: 4RA6), with aspartic acid (Green) (PDB id: 4NJE) and with citrate ion (Magenta) (PDB id: 4RA9). The structural differences at the active site and the flexible loop regions are highlighted with oval (Torquoise) and rectangular (Orange) outlines, respectively.

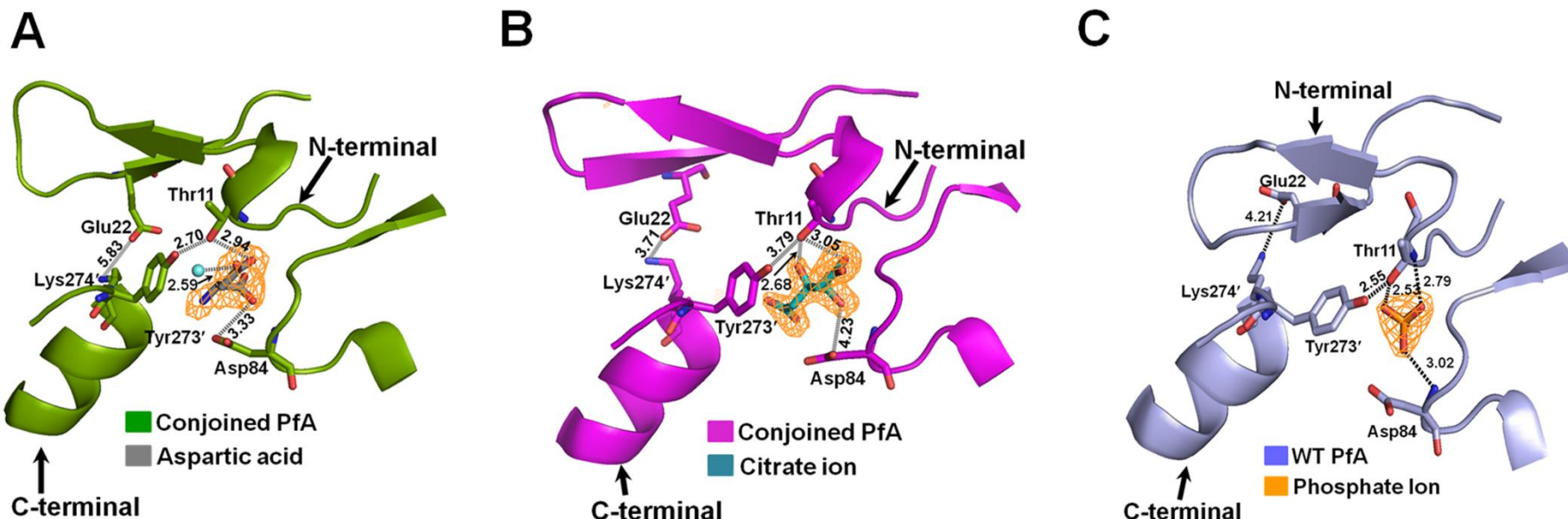


Figure S6 Active site composition of conjoined PfA (complexed with ligands) (PDB id: 4NJE and 4RA9) and WT PfA (with phosphate ion) (PDB id: 4Q0M) at catalytic triad I. Active site residues involved in interaction with aspartic acid (Grey) (**A**) and with citrate ion (Cyan) (**B**), showing stabilized β -hairpin loop of conjoined PfA. Fo-Fc (Orange) contoured at $4.0\ \sigma$ and $5.0\ \sigma$ for placing the ligands respectively, are satisfied. (**C**) Stabilized β -hairpin loop of WT PfA and the active site residues involved in interaction with phosphate ion (Dark orange) are shown for comparison. Fo-Fc (orange) contoured at $4.0\ \sigma$ satisfied by placing phosphate ion.

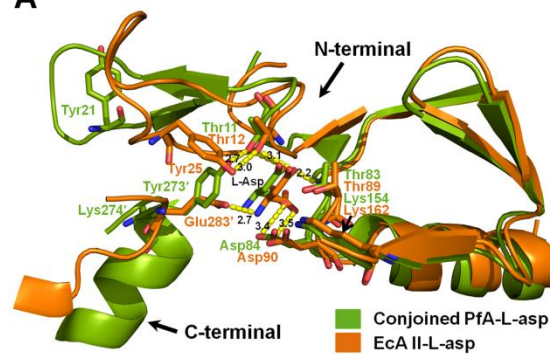
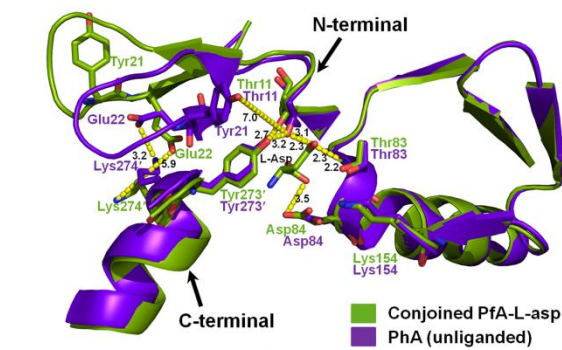
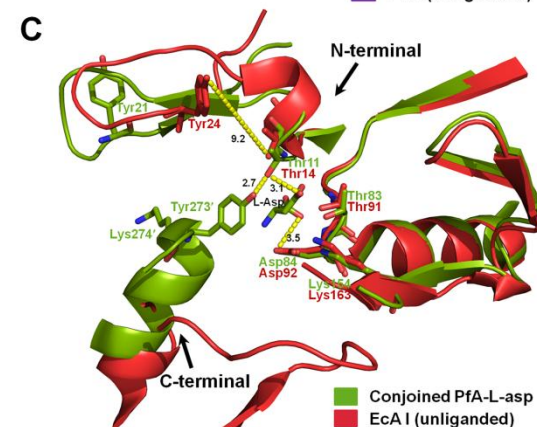
A**B****C**

Figure S7 Comparison of active site and loop region of conjoined L-asparaginase with other type I and type II L-asparaginases. **(A)** Superimposed structures of substrate-bound conjoined PfA (Green) (PDB id: 4NJE) with EcAII (sunlight copper) (PDB id: 3ECA). The Tyr21 of PfA projecting away, while the Tyr273' occupying an equivalent position to the Tyr25 of EcAII constituting the catalytic basic residues is shown. Note that the presence of substrate makes the loop in conjoined PfA stable as a β -hairpin structure; which in EcAII is flexible. **(B)** Superimposed structures of substrate-bound conjoined PfA (Green) (PDB id: 4NJE) with the unliganded PhA (purple blue) (PDB id: 1WLS). Differences in orientation of the Tyr21 residue between these two enzymes and its far away location from the critical active site Thr11 is shown. This minimizes the possibility of Tyr21 to acts as base in both the structures, instead Tyr273' of PhA is also found to align with the conjoined PfA. Note that the distance between Glu22 and Lys274' (3.4 \AA) residues of PhA makes it an important loop stabilizing interaction which is not seen in the case of PfA, where this distance is quite large (5.9 \AA). **(C)** Superimposed structures of substrate-bound conjoined PfA (Green) (PDB id: 4NJE) with the unliganded EcAI (red) (PDB id: 2P2D) showing conserved key active residues Thr14, Thr91, Asp92 and Lys163. Note that in EcAI the Tyr24 residue (equivalent to Tyr25 of EcAII) is far away from the active site whereas the other residue Tyr273' (important in PfA catalysis), is altogether absent from the catalytic centre.

Table S1 The comparison of crystal structures of available bacterial and archeal L-asparaginases.

SN	Organism	Name	Residues	PDB	Taxonomy	Multimericity	Homology (Q _H)	rmsd (Å)	Linker length	Linker Sequence
1	<i>Pyrococcus furiosus</i>	PfA	326	MODEL	Archea	DIMERIC	-	-	19	183-FIPKFNNGEVTLDRHDPK-201
2	<i>Erwinia carotovora</i>	EcrA	327	2GVN	Bacteria	TETRAMERIC	0.64	2.3	23	197-TRLDKVHTTRSVFDVTNVDKLPA-219
3	<i>Campylobacter jejuni</i>	CjA	334	3NXK	Bacteria	TETRAMERIC	0.66	2.3	22	198-NVIKAHTKNAPFDVSKLTSLPK-219
4	<i>Yersinia pestis</i>	YpA	341	3NTX	Bacteria	DIMER	0.66	2.2	21	191-SSVVSPPTSNGPLIVHRITPQP-211
5	<i>Helicobacter pylori</i>	HpA	332	2WT4	Bacteria	TETRAMERIC			24	197-MQPLRKHTTESEFSQLKTPLPK-220
6	<i>Erwinia chrysanthemi</i>	ErA II	327	1HFW	Bacteria	TETRAMERIC	0.65	2.2	23	197-NRIDKLHTTRSVFDVRGLTSLPK-219
7	<i>Escherichia coli</i>	EcA II	326	3ECA	Bacteria	TETRAMERIC	0.65	2.3	22	191-RTPARKHTSDTPFDVSKLNELP-212
8	<i>Escherichia coli</i>	EcA I	358	2P2D	Bacteria	TETRAMERIC	0.66	2.4	21	191-NTPPAPHGEGELEVHPITPQP-211
9	<i>Vibrio cholerae</i>	VcA	337	2OCD	Bacteria	TETRAMERIC	0.66	2.2	22	191-TNVKVDEKPSGEFKVNPITPQP-212
10	<i>Pyrococcus horikoshii</i>	PhA	328	1WLS	Archea	DIMER	0.97	0.27	19	183-HIPDFYGDEFFSDIKYEPK-201
11	<i>Acinetobacter glutaminasificans</i>	AcA	331	1AGX	Bacteria	TETRAMERIC	0.65	2.4	25	193-RSSVKKHTNNSEFNIKEIQGDALPG-217
12	<i>Pseudomonas sp. 7A</i>	PsA	330	1DJP	Bacteria	TETRAMERIC	0.66	2.3	23	201-RLPAKRHTVNSEFDIKQISSLPQ-223

Table S2 Comparison of secondary structural contents.

S/N	Secondary structure contents	Crystal structure information (PDBSUM analysis) (Laskowski, 2009)		Circular Dichroism calculation (Reed's Ref.)	
		WT PfA	Conjoined	WT PfA	Conjoined PfA
1.	α -helix	27.5%	29.78%	32.8 %	26.6%
2.	Strands	46.48%	20.5%	41.9%	29.8%
3.	Others	26.02%	49.66%	25.4%	43.5%

S1. Primer sequences for PCR amplification of PfA domains.**NPfA****Forward Primer:** 5'CT GCT AGC GTG AAA ATT CTT CTA ATT G 3'**Reverse Primer:** 5'AG GGA TCC TTA GTT AAC CAC GAG ATC TTC TC 3'**CPfA****Forward Primer:** 5'TA GCT AGC GTC CTA GTT ATC AAA CTA ATC C 3'**Reverse Primer:** 5' GGC GGG ATC CTA ATC TCT AAG CTC TCC 3'